ELSEVIER

Biophysical Chemistry 84 (2000) 87–98

Biophysical Chemistry

www.elsevier.nl/locate/bpc

Reaction–diffusion waves of actin filament polymerization/depolymerization in *Dictyostelium* pseudopodium extension and cell locomotion

Michael G. Vicker*

Department of Biology and Chemistry, University of Bremen, D-28359 Bremen, Germany

Received 10 September 1999; received in revised form 26 November 1999; accepted 29 November 1999

Abstract

Cell surface movements and the intracellular spatial patterns and dynamics of actin filament (F-actin) were investigated in living and formalin-fixed cells of *Dictyostelium discoideum* by confocal microscopy. Excitation waves of F-actin assembly developed and propagated several micrometers at up to 26 μm/min in cells which had been intracellularly loaded with fluorescently labeled actin monomer. Wave propagation and extinction corresponded with the initiation and attenuation of pseudopodium extension and cell advance, respectively. The identification of chemical waves was supported by the ring, sphere, spiral and scroll wave patterns, which were observed in the extensions of fixed cells stained with phalloidin-rhodamine, and by the similar, asymmetrical [F-actin] distribution in wavefronts in living and fixed cells. These F-actin patterns and dynamics in *Dictyostelium* provide evidence for a new supramolecular state of actin, which propagates as a self-organized, reaction–diffusion wave of reversible F-actin assembly and affects pseudopodium extension. Actin's properties of oscillation and self-organization might also fundamentally determine the nature of the eukaryotic cell's reactions of adaptation, timing and signal response.

Keywords: Actin; Cell locomotion; Oscillations; Chemotaxis; Confocal microscopy; Reaction–diffusion waves; *Dictyostelium*

* Tel.: +49-421-218-4952; fax: +49-421-218-4042.
E-mail address: vicker@uni-bremen.de (M.G. Vicker)

0301-4622/00/$ - see front matter
PII: S0301-4622(99)00146-5

1. Introduction

The form, surface texture and pseudopodial dynamics of *Dictyostelium* cells, like motile eukaryotic cells generally, give an uncanny impression of incoherence, yet they are determined by ordered travelling and stationary waves of various sizes, arising from and decomposing into less ordered, possibly chaotic, patterns at seemingly irregular intervals [1]. Spatio-temporal analysis of these wave dynamics, using circular mapping and primary component analysis, has demonstrated that cells vibrate at several basal frequency modes [2] and, consequently, locomotion is non-random [1,3]. However, the molecular basis of this oscillatory behavior has not been described.

The crawling locomotion of eukaryotic cells requires the projection of filopodia, pseudopodia or lamellipodia, coupled to subsequent cytoplasmic flow, although relatively little attention has been given to this latter point (however, see, e.g. Wessels et al. [4] and Stossel [5]). Projection is based on the assembly and disassembly of actin filaments (F-actin): an autonomous reaction [6], modulated in cells primarily by the regulation of the actin monomer (G-actin) concentration by sequestering proteins, especially profilin [7], and by the inhibition and amplification of filament assembly, chiefly by the actin-binding protein ADF/cofilin [8,9]. However, the mechanism of actin-based cell locomotion is poorly understood. A suggested role for muscle-like actinomyosin dynamics [10] has been contradicted by the locomotive ability of myosin II-null mutants [11]. A number of current proposals attribute the cell's ability to produce locomotory projections to the steady-state regulation of F-actin meshwork and filament dynamics by actin-binding proteins (ABP) at the cell periphery, e.g. by F-actin synthesis, nucleation and branching [12,13], hygroscopic swelling [14], filament treadmilling [15], polar growth [16] and actomyosin-induced contraction and G-actin flux through the mesh [5]. However, cell motility persists, although defective to some degree, after the disablement of genes for ABPs suspected of having key locomotory functions (e.g. [11,17,18]). Consideration of the critical spatio-temporal differences between the stages and locations of F-actin polymerization, cell projection and the filament bundling, linking or contraction activities proposed for ABPs might help resolve some of these issues.

Dictyostelium discoideum has been extensively used in studies of locomotion, chemotaxis, morphogenesis and cell communication. Recently, we reported [19] that particular spatial patterns of F-actin in formaldehyde-fixed cells correspond in detail to the patterns generated by relaxation oscillations observed in various chemical systems, e.g. the Belousov–Zhabotinsky reaction [20]. The chemical wave-specific features of *Dictyostelium*'s F-actin patterns included, inter alia, spheres, rings, salinon and target forms, rotating spirals, mirror-symmetrical spiral pairs and apparent wave collisions and mutual annihilation of the wavefront segments involved. The patterns represented physical and optical cross-sections of the consecutive developmental stages of wave evolution from spherical to scroll waves and their decay to extinction. In addition to these investigations, a study was conducted of *Dictyostelium*'s reaction to a pulse of its natural chemoattractant cyclic AMP (cAMP). Cyclic AMP induced cells to transiently round up by phase-shifting cell form to oscillation mode 0 and obliterating all F-actin wave patterns within seconds during a massive, sub-cortical F-actin repolymerization [21,22]. During the deadaptation time of this actin reaction, a damping oscillation of synchronous F-actin wave generation developed with basal periods of 6–7 s and 12 s. Fourier analysis and Markov simulation of these dynamics indicated that the F-actin wavefronts induced during these synchronous events propagated at 3.1–17.5 μm/min [19].

Several oscillations and chemical excitation waves in cell and tissue systems have been investigated as examples of self-organization and nonlinear dynamics inherent in reactions far from equilibrium, e.g. in fish skin patterning [23], heart [24] and neuronal tissue [25] electrical activity, cardiocyte [26] and oocyte [27,28] [Ca^{2+}], tubulin polymerization [29], yeast glycolysis and patterns of morphogenical aggregation in *Dictyostelium* amoebae populations [30]. However, despite their ubiquity, these are disparate examples and, thus, the functional relevance of self-organization to

cells and organisms has remained generally obscure, at least in relation to what may be considered basal or fundamental eukaryotic cell functions.

Here, I report observations of the dynamics of cell surface and of autowaves of reversible actin filament assembly, a new supramolecular state of actin, for the first time in a living cell. The results provide evidence that pseudopodium extension and cell locomotion depend on F-actin assembly wave propagation. The possible role of actin is discussed in relation to adaptive reactions, such as chemotaxis.

2. Methods and materials

2.1. Cell culture and video microscopy

Aggregation-stage *Dictyostelium* AX2 cells were grown 48 h axenically in HL-5 nutrient media in stirred suspension [31]. Aggregative NC4 wild type cells were grown 45 h on nutrient agar with *Escherichia coli* as food [19]. Cells were harvested by centrifugation and washed in 17 mM phosphate buffer (KK_2), pH 6.5. For video microscopy [1], a 40 × /1.3 n.a. objective (Zeiss, Oberkochen) was focussed at the dorsal cell surface, which was illuminated acentrically.

2.2. Actin incorporation and confocal microscopy of living cells

Cells were loaded with a mixture of G-actin labeled with Cyanine3.18 (excitation = 554 nm, emission = 565 nm), a kind gift of L. Machesky, Birmingham, UK, and Oregon Green (ex511/em530 nm: Molecular Probes, Eugene, OR, USA) on ice in the dark using 30 electrophoretic pulses (99 ms, 250 V: Model Z 1000, GCA/Precision Scientific Group, Chicago, IL, USA) within 1 min followed by repeated vigorous trituration through a tuberculin needle for 1 min. The actin for Oregon Green conjugation was isolated from rabbit muscle by NH_4SO_4 precipitation [32] and covalently bound to the dye according to the manufacturer's instructions. A total of 10^4 washed cells in 2 ml 5 mM $MgCl_2$ were plated onto a clean glass coverslip glued to a hole bored through the floor of a 35-mm ∅ plastic Petri dish. Split images were recorded in 1.08 s at 3-s intervals using a 40 × objective mounted on an inverted Zeiss LSM 410 confocal microscope operating in the laser transmission mode and at em488/em570

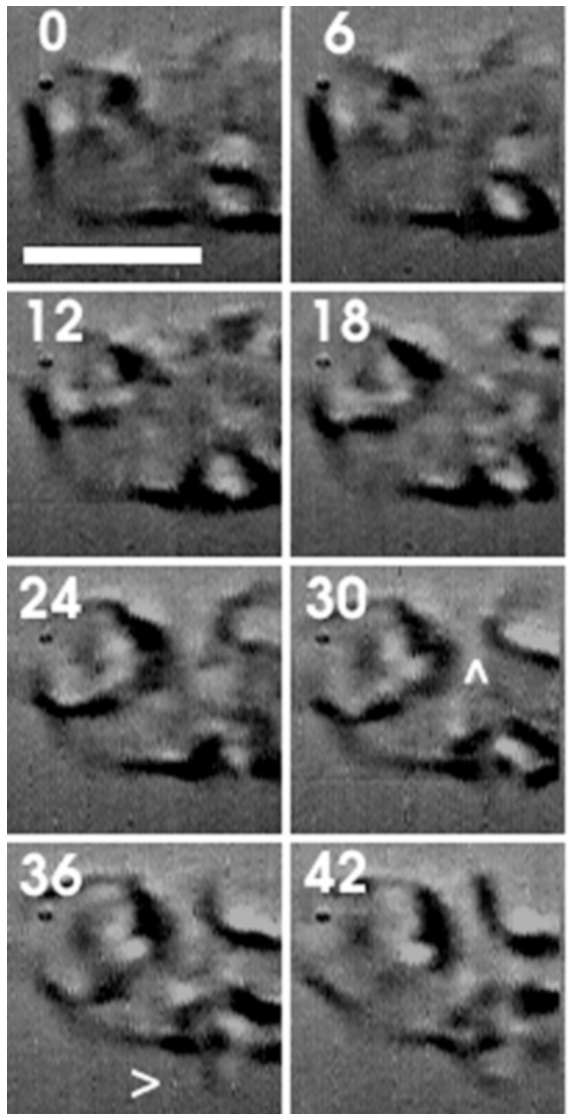

Fig. 1. Waves traverse the upper surface of a live *Dictyostelium* AX2-strain cell. Two waves cease propagation where their fronts approach at 30 s (arrowhead). A third wave, below, extends as a small pseudopodium after 30 s (arrowhead). The bar represents 10 μm. Time in seconds is displayed in each frame.

nm for fluorescence resonance energy transfer (FRET). The confocal image plane was selected slightly above the glass substratum in order to reduce background fluorescence.

2.3. Confocal microscopy of fixed cells

Cells, locomoting on glass in KK_2, were fixed in 3.7% formaldehyde overnight, washed three times in KK_2 and stained with 0.8 μM phalloidin-tetramethylrhodamine-isothiocyanate (Sigma, Diesenhof) in the same buffer for 1 h [1]. The cells were washed three times in KK_2 and mounted in glycerol/KK_2 (4:1). Confocal images were obtained using a Leica TCS4D system operating to record TRITC emission. Digital images were prepared using Adobe Photoshop software 3.0. Pixel intensity scans of the video images were made using NIH Image 1.67 software for Macintosh.

3. Results

3.1. Cell surface observations

The protrusive activity of the *Dictyostelium* cell surface includes circular wavefronts, which have been noted as 'food cups' [33] or F-actin-containing 'crowns' [9,34] and pseudopodia. Circular waves are common features, which may continue as pseudopodia near the cell periphery (Fig. 1). However, two wavefronts halt at their closest approach before collision, indicating the possibility of mutual interaction. Waves propagate several micrometers at a range of rates (Fig. 2) similar to those reported for *Dictyostelium* cell speed (e.g. [4,35]).

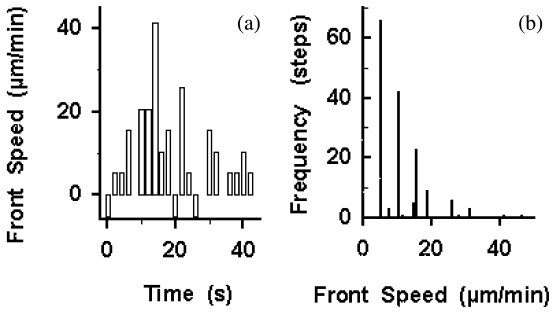

Fig. 2. Cell surface wave behavior. (a) The speed of one cell surface wave recorded from the film used in Fig. 1 every 2 s. (b) Positive wave velocities (speed per time step interval) recorded on the surfaces of 12 cells.

3.2. F-Actin in live Dictyostelium

The behavior of fluorescently labeled F-actin, tracked within living cells, allows analysis of cell surface and pseudopodial dynamics at the molecular level. An F-actin wavefront may be followed through a virtually complete developmental sequence from nascence to disintegration in under 12 s (Fig. 3). The large fluorescent signal visible near the center of the cell might be due to sequestered G-actin, because its intensity decreased in a later image sequence, although autowave development continued. Initially, a small,

Table 1
F-Actin wavefront dimensions and propagation rates in a live *Dictyostelium* NC4-strain cell

Image (s)	Wave outer Ø ave. (μm)	Rim width ave. (μm)	Wavefront speed (μm/min)			Cell anterior speed (μm/min)
			Center	Ave.	Front	
0	1.38	0.69[a]	–	–	–	–
3	1.90	0.95[a]	0	5.2	2.4	2.4
6	3.59	1.32	0	17.0	12.2	14.0
9	4.95	1.14	19.4	13.1	45.8	38.8
12	4.28	0.85	33.8	3.4	7.4	26.6

[a] The value is that of the F-actin area radius only. 'Wave outer Ø', 'rim width' and 'wavefront speed' each indicate an average of two or four measurements of the wavefront in the *x* and *y* directions relative to the geometrical F-actin ring or area center. Forward speeds were recorded at (1) the geometrical F-actin area or ring 'center'; (2) the wave's leading, anterior margin ('front'); and (3) the 'cell anterior', i.e. the leading tip of the pseudopodium. The data were gathered from Fig. 3.

immobile F-actin patch, located immediately behind the cell's leading margin, decreased in amplitude from 0 to 3 s. Between 3 and 6 s, more F-actin became incorporated into a faint ring (below the oblique bracket), which subsequently expanded and became fragmented by 9 s. Decay was essentially completed by 12 s. Surviving wavefront fragments became radially arrayed ('spokes'), normal to the cell margin the previous and wavefront: an F-actin pattern found, for example, in neutrophils [16] and fibroblast actin

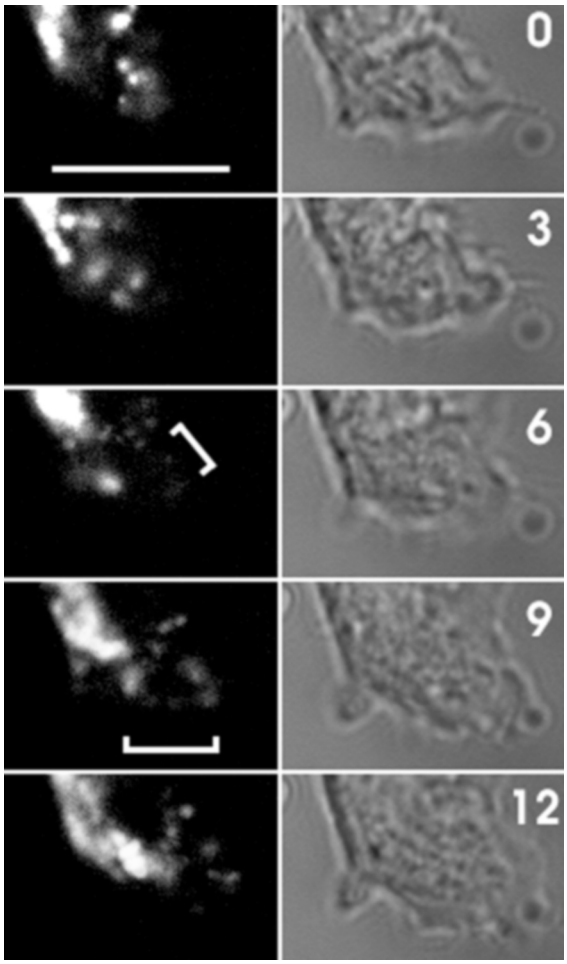

Fig. 3. An F-actin wave propagating within a living *Dictyostelium* NC4-strain cell. A sequence of five split-screen confocal fluorescence and laser transmission image pairs were recorded at 3-s intervals. The ring developing at 6 and 9 s is indicated by brackets. The bar indicates 10 μm. Time in seconds is displayed in each frame pair.

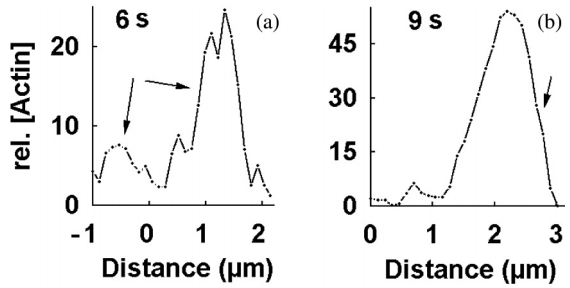

Fig. 4. Plots of the relative F-actin concentrations of wavefronts in Fig. 3. (a) A pixel intensity plot of the ring at 6 s. The bracket in Fig. 3 indicates the extent and direction of the plot across both wavefronts (arrows): diagonally, left to right. (b) A plot of half of the ring at 9 s, scanned from the ring center across the anterior wavefront on the right. The wavefront (arrow) is steeper than the back of the wave. The intensity scale 0–255 corresponds to black–white.

rings [36]. Propagation speed increased as the ring expanded and decreased as it approached extinction (Table 1). The maximum velocity of the leading sector of the wavefront reached 45 μm/min at 6–9 s. However, local cytoplasmic flow, registered in the apparent 19 μm/min advance of the center of the ring, might have added to this value. The pseudopodium rate of advance subsequently increased to 39 μm/min by 9 s. The correspondences in speed and mutual timing between wavefront and pseudopodium advance of both indicate that the F-actin wave governed the pseudopodial events depicted in the image sequence. The F-actin concentration plots of these images demonstrate that the pattern at 6 s is indeed ring-shaped, although unequally distributed, and that the wavefront rims at 6 and 9 s are asymmetrical (Fig. 4).

3.3. F-Actin patterns in fixed cells

The high rates of cell locomotion and F-actin wavefront propagation, as well as the sensitivity of cells to light, restricted image quality and the time available for optical sectioning in living *Dictyostelium* cells. Confocal microscopy of fixed cells, specifically labeled for F-actin, demonstrated three-dimensional details of the shapes and dimensions of wavefronts similar to that in Fig. 3. In some cells, pseudopodia contained one large,

flat F-actin ring or a nascent F-actin sphere (Fig. 5a,b). Such rings are liable to deteriorate to spirals (Fig. 5c,d). Spirals develop from the free ends of broken wavefronts and each rotates about a small, axial, unexcitable vortex region (arrowhead) [20,37]. A contour plot of this image demonstrates its spiral morphology (Fig. 6). The remnants of two putative spirals at each end of a bipolar cell consist of a filigrane of miniscule, hollow F-actin spheres (Fig. 5e–i). One cross-section of the cell in Fig. 5j (in the plane indicated by the arrowhead) shows that the large ring is in fact a sphere

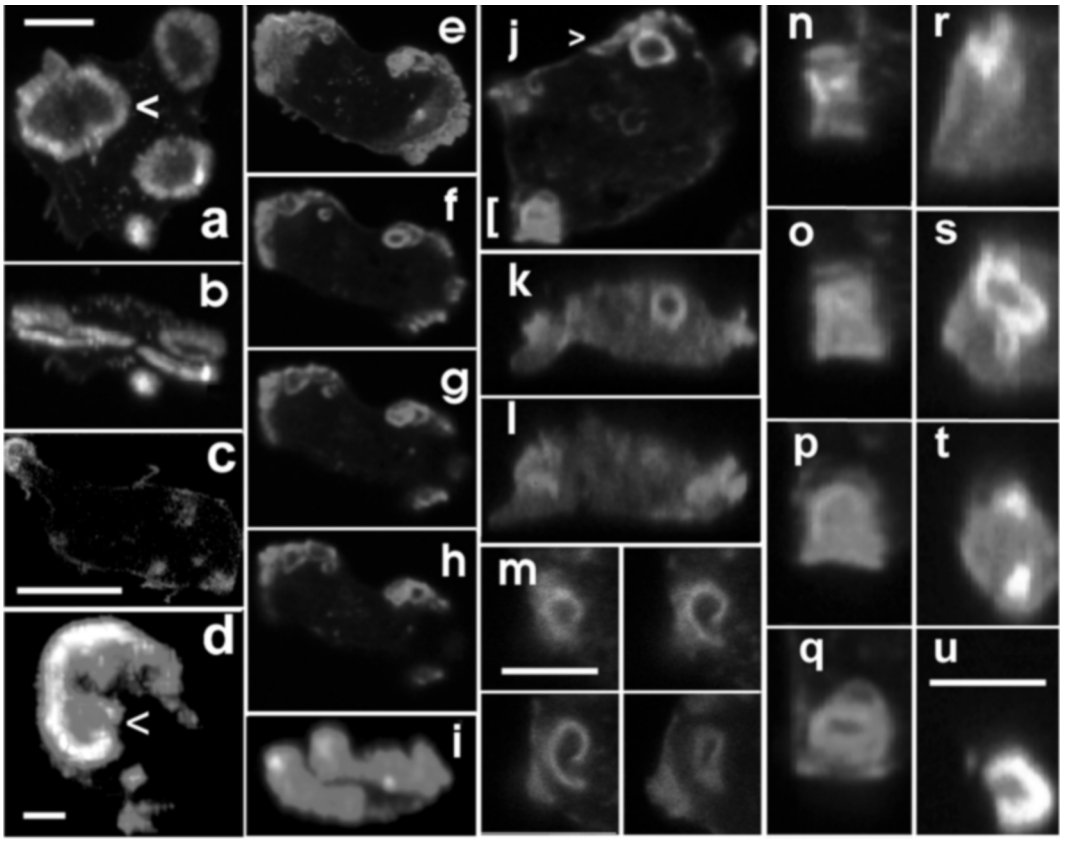

Fig. 5. Confocal image series and reconstructions of F-actin wavefronts in formaldehyde-fixed *Dictyostelium* cells. (a) A *z*-axis reconstruction of 46 optical sections of an AX2 cell. The dorsal aspect shows four F-actin waves in various stages of development each within one pseudopodium. (b) The thinness of each F-actin ring is demonstrated by a rotation view of nearly 90°. (c) A single section through a NC4 cell shows a spiral wave at the tip of one pseudopodium (d). A three-dimensional reconstruction of the wave from 70 vertical sections shows a spiral and vortex region (arrowhead). (e) A reconstruction of 50 optical sections through a bipolar AX2 cell showing two wavefronts composed of a filigrane pattern of F-actin rings. (f–h) Three confocal sections of the cell, ventral to dorsal, 0.2 μm apart, indicate the F-actin ring patterns. Some 'spokes' appear to be rings viewed laterally. (i) A *z*-axis reconstruction of the image in (e) viewed from the left and rotated 90° showing the three-dimensional nature of the actin fronts. (j) An optical median section through an AX2 cell. (k–l) Two vertical sections through this cell, 0.6 μm apart, show that the ring (j, arrowhead) is a spherical wavefront and that the upward projection from the substratum at the right in (j) is a pseudopodium containing a scroll wave of F-actin, which appears in cross-section as two partial rings. (m) Four sections through a spiral in a pseudopodium of another cell show that the F-actin pattern may be a segment of a scroll wave extending at least 3 μm. The first three sections are 0.2 μm apart and the fourth is 2.0 μm below. (n–q) Four horizontal sections through the top half of the small pseudopodium at the lower left of the cell in (j), beginning at the dorsal cell surface. (r–u) Four cross-sections 0.6 μm apart through the same region in (j, bracket), in a direction toward the cell margin, show a scroll wave. The bar in (a) indicates 5 μm for (a,b,e–l), that in (c) 5 μm, that in (d) 0.5 μm, that in (m) 5 μm, and that in (u) 5 μm for (n–u).

Fig. 6. A contour density plot of the F-actin spiral at the front of the pseudopodium in Fig. 5d.

(Fig. 5k). A second cross-section shows a small scroll wave within a pseudopodium, projecting at the right above the substratum (Fig. 5l). Fig. 5m shows a spiral in a pseudopodium of a cell. The spiral extends vertically at least 3 μm and might be a segment of a scroll wave. Another extension of the cell in Fig. 5j contains a complete F-actin scroll wave sectioned horizontally (Fig. 5n–q) and cross-sectioned (Fig. 5r–u). Note that neither 'ring' in Fig. 5o is closed. The scroll wave is oriented with its central axis parallel to the substratum and is symmetrical but irregular, being narrower above and below. A model of a scroll wave (Fig. 7) has been cross-sectioned at four equidistant points and shows patterns virtually identical to those in Fig. 5r–u. Densitometric measurements of wavefronts in living (Fig. 3) and fixed cells (Fig. 5a,e,j) consistently demonstrate sharp leading margins trailed by relatively flatter [F-actin] gradients (compare Fig. 4a,b with Fig. 8a–c).

4. Discussion

4.1. Reaction–diffusion wave properties

The F-actin patterns of active wavefronts in both living and fixed cells probably originate by autowave propagation. Alternative mechanisms of formation have either been discounted, e.g. spherical pattern development on intracellular vesicles [19], or lack a chemical or biophysical precedent. It is probably unnecessary to assume a qualitative difference in the molecular reactions at actin filament ends, which occur during the formation of these patterns and waves or during the formation of filaments in meshworks or bundles. However, such a difference distinguishes the dynamics and form of chemical waves from the formation of actin, filaments and bundles: the former proceeding as a global, self-organized reaction. Thus, chemical waves of reversible actin polymerization demonstrate a new supramolecular state or behavior of actin which has not been previously identified.

The wavefront velocity, diameter and rim width in Fig. 3 are consistent with values obtained for F-actin circular waves from *Dictyostelium* cells fixed after exposure to a pulse of cAMP [19]. F-Actin density plots also demonstrate a similar asymmetrical concentration distribution across wavefronts in living and fixed cells. Asymmetry may indicate the reaction–diffusion nature of such wavefronts, because it is consistent with the three main states necessary for the propagation of relaxation waves as described in chemical systems [20,38,39]: (1) an unstable and excitable state of the medium; (2) nucleation of the reaction and its autocatalytic propagation; and (3) a trailing, refractory zone of relaxation and regeneration. This three-phase pattern is represented in propagating chemical waves, for example, like the front of a dry grass fire, and is similar to the F-actin dynamics in *Dictyostelium*. The requirement for an

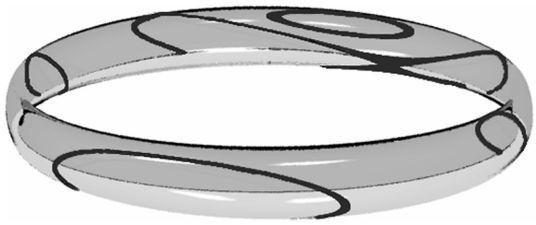

Fig. 7. A scroll wave model of the F-actin patterns in Fig. 5r–u. The model is viewed from the pseudopodium's distal tip and has been rotated 90° relative to the original data. Two segments of the scroll are relatively thinner (left and right), like those of the scrollwave in the cell. Four cross-sections through the clear model generate patterns similar to those of F-actin in each of the four sections of the cells.

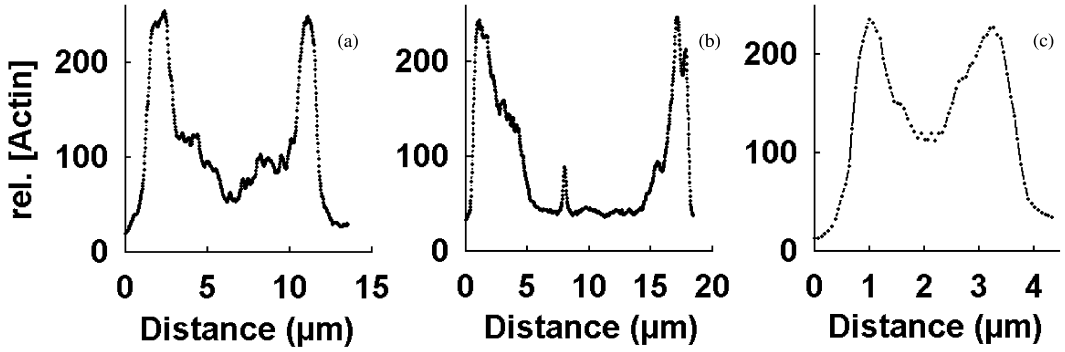

Fig. 8. F-Actin concentration and distribution plots from three wavefronts in Fig. 5. Pixel intensity plots were made across (a) the large ring wavefront in Fig. 5a (arrowhead), (b) across the whole cell in Fig. 5e (left to right), and (c) across the ring in Fig. 5j (left to right).

excitable medium is fulfilled by cytoplasm containing G-actin$_{ATP.}$ The propagating wavefront may consist of F-actin nucleation and assembly into oligomeres which fragment to initiate new filament assembly. The front might propagate with a high rate of filament assembly and disassembly and a low rate of diffusion of the longer filaments. The zone of relaxation and regeneration distal to this wavefront consists of filaments undergoing disassembly and dispersion after which ADP is exchanged for ATP in G-actin. Relaxation may involve two chief parameters: (1) the random or cooperative hydrolysis of F-actin-bound ATP [40]; and (2) the probability that cofilin activity may be necessary to amplify both filament and nucleation site number in propagating waves by producing severed filaments, which might provide either free ends for polymerization or disintegrating fragments. Filament amplification would prevent waves from thinning-out to extinction during wavefront expansion. This point is supported by the observation that the [F-actin] appears broadly similar in wavefronts of various sizes [19]. Fluorescently labeled cofilin in living *Dictyostelium* cells has been located in rapidly-forming ring-shaped patterns [9], much the same in appearance and dynamics as the F-actin patterns described above, and consistent with a close association between cofilin and F-actin wavefronts.

4.2. Wave induction and interactions

Small GTP-binding proteins such as Rho and Rac (reviewed by Hall [41]) and tyrosine kinases [42] transmit signals leading to F-actin synthesis and the extension of filopodia, F-actin stress fibers or ruffled membrane activity, respectively, in different cell types. However, the role of these signal pathways in *Dictyostelium* cell locomotion and chemotaxis is unclear. Autonomously motile cells require neither extracellular agonists nor contact with the substratum and F-actin wave propagation may proceed at some distance from the plasma membrane and, thus, signals emanating from it. *Dictyostelium* null mutants for the RasG GTPase retain the abilities of autonomous motility and chemotaxis to an oriented folic acid pulse [43]. It may be worth considering the role of the small GTPases in cell motility in relation to their order of appearance in the sequence of events after cell stimulation. Cyclic-AMP-induced reactions in *Dictyostelium* demonstrate two different effects on actin. The first is an immediate (1–6 s) adaptive, sub-cortical F-actin assembly reaction [21]. During this reaction, F-actin waves are eliminated and their formation inhibited for nearly 20 s, possibly by a reduction in the availability of sufficient G-actin for wave propagation. The second effect occurs during deadaptation to the agonist. F-Actin waves subsequently appear, but in synchronous, rhythmical events of propagation and extinction [19]. These points raise the possibility that the agonist-induced reactions and F-actin waves are interdependent, but regulated differently. Although cAMP affects F-actin wave

dynamics and pseudopodium formation, e.g. in chemotaxis, the effect on pseudopodia production might be indirect and related to the competition for free G-actin$_{ATP}$ among a population of surviving nucleation sites, leading to rhythmic wave formation and extinction as the G-actin supply becomes available or exhausted in an inverse, damping rhythm. After deadaptation to the agonist, the synchrony and periodicity of these F-actin wave dynamics are lost, but cell locomotion continues. The spatio-temporal pattern of developing waves in a cell might also be determined by competition for G-actin. Such communication, interference or interdependence between propagating waves are aspects of self-organization.

Although chemical waves are unlikely to directly force the plasma membrane forward, it seems probable that they induce other local reactions which do, much like the hydrodynamic flow generated at the front of exposed Belousov–Zhabotinsky reaction waves [44]. Pseudopodia which extend, but fail to induce flow, wither rapidly and have little or no apparent locomotory effect (M.G. Vicker, unpublished observations). Differentiation of process extension and subsequent induced flow of the cell into it might help identify the roles and relative periods of activity of actin and ABPs. Thus, it is tempting to speculate that the generation of F-actin mesh might occur immediately after wave passage.

4.3. Wavefronts in living and fixed fibroblasts and amoebae

F-Actin waves are usually not found in reports in which detergent was included during cell fixation. Fixation in the presence of detergent destroyed all F-actin wave patterns in *Dictyostelium* (data not shown). This observation might help differentiate the F-actin in waves from ABP-containing meshworks and it might also indicate the oligomeric nature of wavefront actin. Actin filaments in *Dictyostelium* are short: averaging 76 monomers (200 nm) in length [45]. F-Actin rings have been noted in projections of fixed *Dictyostelium* (e.g. [8,43]) and vertebrate tissue culture (e.g. [36,46,47]) cells. We have previously interpreted these and similar patterns as F-actin autowaves [1,19]. Fluorescent F-actin has been monitored in living *Dictyostelium* cells [48–51], however, these studies have shown no evident dynamical actin organization or pattern and therefore they presented no information about actin's role in the mechanism of cell locomotion. Studies of fixed and stained amoebae species have lead to the suggestion that their locomotory mechanism and actin organization differs from those of *Dictyostelium* [52].

F-Actin has been observed in living fibroblasts and keratinocytes after cell loading with fluorescently labeled G-actin (e.g. [15,53–55]). There was no consistent correlation between the dynamics of actin, lamellipodium extension and cell advance, although the results indicated some form of actin filament turnover at the leading cell margin. However, Ballestrem et al. [56] have recently transformed melanoma cells with an actin-green fluorescent protein (gfp) fusion protein and recorded what may be interpreted as F-actin wavefronts in living cells, i.e. developing ring pairs and mirror-symmetrical spirals (i.e. sections of a scroll wave), although the authors described them as 'actin clouds'. The F-actin wavefronts in these cells expanded and deteriorated in emergent lamellipodia within 15 min vs. 12 s for *Dictyostelium*. Their images were used to calculate the melanoma cell F-actin wavefront speed and lamellipodial extension rates both at 1.7–2.3 μm/min, i.e. a rate approximately 20-fold slower than the maximum rate of *Dictyostelium* cell and actin wave advance.

Ruffled membranes are typical, F-actin-containing features of lamellipodia [57], but their origin has not been elucidated. It is possible to suggest that ruffled membranes arise from the retrograde propagation of F-actin wavefront segments as anterior segments drive lamellipodium extension forward. Similarly, the origin of *Dictyostelium*'s expanding circular surface waves may depend on underlying F-actin waves.

4.4. F-Actin waves, oscillations and eukaryotic cell behavior

F-Actin wave patterns in living and fixed *Dictyostelium* and melanoma cells qualitatively corre-

spond in size, form and dynamical behavior. The temporal relationship between wave activity and cell margin advance is close in *Dictyostelium* and identical in melanoma cells [56]. The evident correspondence between cause and effect suggests that F-actin waves may be the primary mechanism for lamellipodia and pseudopodia extension. Some ABPs might modulate this basic function depending on range of locations and timing of their activity within an active extension. ABPs might modulation wave speed and frequency, perhaps eliciting the differences between developing amoebae [58] or cell types, or they might bind and/or induce rapid F-actin assembly after local wave passage, e.g. F-actin binding to myosin II occurs at the non-motile cell pole [59,60].

The non-linear and self-organizational properties of F-actin waves and oscillations might also be fundamental for eukaryotic cellular behavior, because many other key molecular systems are coupled to or react with actin. For example, some cell surface signal receptors and ion channels have been reported coupled to actin [61–65]. It would be interesting to learn whether the dynamics of these systems is modulated by actin oscillations. A second possible example rests on the adaptive and oscillatory reactions of actin to extracellular signals. By alternating between different phase states of reactivity and refractoriness, actin might either gate or modulate a coupled reaction system to which it is engaged. Although other cellular oscillators may also exist, e.g. comparatively regular oscillations in various immune functions which might be independent of an actin oscillator have been reported in neutrophils [66,67], actin is functionally coupled to key cellular activities. Thus, *Dictyostelium* cell motility is sensitive to the [cAMP] in a triphasic manner, which possibly reflects differences induced in F-actin wave frequency or intensity, a point requiring further investigation. Other cellular physiological reactions to the [cAMP] or to a spatial gradient of cAMP (one lacking temporal development) besides these are unknown. This particular reaction induces cells to migrate by random locomotion either up or down the gradient and accumulate (by trapping) within attractant concentrations in which they are relatively less motile [35,68]. However, a cAMP pulse induces a qualitatively and quantitatively different response involving a wide range of physiological reactions in addition to transient plasma membrane-associated F-actin polymerization, F-actin wave dissolution (i.e. wave phase resetting) and subsequent regular oscillations in F-actin wave generation, during which time the cell deadapts to the cAMP signal. The mechanism by which an oriented pulse orients the cell's response, may be postulated to depend on the phase resetting, which begins at the initial point of cAMP wave contact. Depolymerization of the plasma membrane-associated F-actin cortex initiated at this point may then establish the position of the first post-cAMP-signal actin wave and, thus, the direction of the next pseudopodium [1]. This example illustrates how adaptive reactions arising out of actin's temporal reaction properties might be necessary for the cell to perceive the direction of a cAMP temporal signal and couple it to the cytoplasm's locomotive machinery. It also provides a molecular mechanism for chemotaxis (i.e. oriented cell turning to an oriented signal) by explaining why pseudopodia projection towards an attractant signal pulse is initiated 30 s after signaling begins, how the projection is oriented, and how cells might distinguish temporal signals of differing attractant concentrations (e.g. an isotropic or spatial gradient) and differing frequencies, i.e. frequency coding [69]. These conclusions contradict those of Parent and Devreotes [70], that chemotaxis depends on a cAMP spatial gradient. The authors treated *Dictyostelium* cells with a developing gradient of cAMP and recorded the aggregation of the cytosolic regulator of adenylyl cyclase (CRAC) at the leading pseudopodium. A film of these events (www.sciencemag.org/feature/data/990801.shl) shows that CRAC oscillates at the plasma membrane with an average period of 40 s (my observations) in each cell, indicating that the cells were not exposed to a cAMP spatial gradient alone. The exclusive application of cAMP pulses is unlikely to distinguish the effects of temporal signals from those of static spatial gradients. What role CRAC might have in cell locomotion and orientation is also unclear.

The temporal characteristics of actin oscillations might facilitate cellular timing operations, and induced frequency differences in them might also regulate cell behavioral differences, e.g. motility, differential taxis and sorting out, which each ultimately depend on actin dynamics. For example, during morphogenesis, *Dictyostelium* cell populations split into two major subgroups with basal oscillation frequencies of 8 and 16 min [58]. These frequencies, which are expressed as differences in actin oscillations, appear to determine cell behavioral differences, reflected in the emergence of subpopulation positioning and the polarity and locomotion of the developing slug [71]. The determination of cell differentiation and morphogenic behavior in developing tissue by actin-associated frequency difference between cell subpopulations is an attractive idea in various systems.

Acknowledgements

Cyanine3.18-labelled actin was kindly provided by L.M. Machesky, Biochemistry, Birmingham, UK. I am indebted to C. Aumann-Kopp, Production Technique, Bremen, for helping to construct Fig. 7 using Deskartes 3.2 software for a Silicone Graphics Workstation.

References

[1] T. Killich, P.J. Plath, W. Xiang, H. Bultmann, L. Rensing, M.G. Vicker, J. Cell Sci. 106 (1993) 659.
[2] T. Killich, P.J. Plath, E.-C. Haß et al., BioSystems 33 (1994) 75.
[3] R.S. Hartman, K. Lau, W. Chou, T.D. Coates, Biophys. J. 67 (1994) 2535.
[4] D. Wessels, J. Murray, D.R. Soll, Cell Motility Cytoskeleton 23 (1992) 145.
[5] T.P. Stossel, Blood 84 (1994) 367–379.
[6] P.A. Dufort, C.J. Lumsden, Cell Motility Cytoskeleton 25 (1993) 87.
[7] A.A. Noegel, J.E. Luna, Experientia 51 (1995) 1135.
[8] H. Aizawa, K. Sutoh, I. Yahara, J. Cell Biol. 132 (1996) 335.
[9] H. Aizawa, Y. Fukui, I. Yahara, J. Cell Sci. 110 (1997a) 2333.
[10] H.E. Huxley, Nature (London) 243 (1973) 445.
[11] D. Wessels, D.R. Soll, D. Knecht, W. Loomis, A. Delozanne, J. Spudich, Dev. Biol. 128 (1988) 164.
[12] M.D. Welch, A.H. Depace, S. Verma, A. Iwamatsu, T.J. Mitchison, J. Cell Biol. 138 (1997) 375.
[13] R.D. Mullins, J.A. Heuser, T.D. Pollard, Proc. Natl. Acad. Sci. USA 95 (1998) 6181.
[14] J. Condeelis, Annu. Rev. Cell Biol. 9 (1993) 411.
[15] Y.-L. Wang, J. Cell Biol. 101 (1985) 597.
[16] T. Redmond, S.H. Zigmond, Cell Motility Cytoskeleton 26 (1993) 7.
[17] W. Witke, M. Schleicher, A.A. Noegel, Cell 68 (1992) 53.
[18] F. Rivero, R. Furukawa, A.A. Noegel, M. Fechheimer, J. Cell Biol. 135 (1996) 985.
[19] M.G. Vicker, W. Xiang, P.J. Plath, W. Wosniok, Physica D 101 (1997) 317.
[20] A.T. Winfree, S.H. Strogatz, Nature (London) 311 (1984) 611.
[21] J. Condeelis, A. Hall, A. Bresnick et al., Cell Motility Cytoskeleton 10 (1988) 77.
[22] G.N. Europe-Finner, B. Gammon, C.A. Woodand, P.C. Newell, J. Cell Sci. 93 (1989) 585.
[23] S. Kondo, R. Asai, Nature (London) 376 (1995) 765.
[24] A.T. Winfree, Science (Washington DC) 266 (1994) 1003.
[25] A. Fuchs, J.A.S. Kelso, H. Haken, Int. J. Bifurcation Chaos 2 (1992) 917.
[26] P. Lipp, E. Niggli, Biophys. J. 65 (1993) 2272.
[27] H.Y. Kubota, Y. Yoshimoto, M. Yoneda, Y. Hiramoto, Dev. Biol. 119 (1987) 129.
[28] J.D. Lechleiter, D.E. Clapham, J. Physiol. 86 (1992) 123.
[29] E. Mandelkow, E.-A. Mandelkow, H. Hotani, B. Hess, S.C. Müller, Science (Washington DC) 246 (1989) 1291.
[30] S.C. Müller, T. Mair, O. Steinbock, Biophys. Chem. 72 (1998) 37.
[31] M.M. Sussman, Methods Cell Biol. 28 (1987) 9.
[32] L.M. Machesky, A. Hall, J. Cell Biol. 138 (1997) 913.
[33] C. de Chastellier, A. Ryter, J. Cell Biol. 75 (1977) 218.
[34] E.L. de Hostos, B. Bradtke, F. Lottspeich, R. Guggenheim, G. Gerisch, EMBO J. 10 (1991) 4097.
[35] M.G. Vicker, J. Cell Sci. 107 (1994) 659.
[36] P. Blume-Jensen, L. Claesson-Welsh, A. Siegbahn, K.M. Zsebo, B. Westermark, C.-H. Heldin, EMBO J. 10 (1991) 4121.
[37] B.J. Welsh, J. Gomatam, A.E. Burgess, Nature (London) 304 (1983) 611.
[38] M. Gerhardt, H. Schuster, J.J. Tyson, Physica D 50 (1991) 189.
[39] S.K. Scott, K. Showalter, J. Phys. Chem. 96 (1992) 8702.
[40] T. Ohm, A. Wegner, Biochim. Biophys. Acta 1208 (1994) 8.
[41] A. Hall, Science (Washington DC) 249 (1990) 635.
[42] Y. Wang, J. Liu, J.E. Segall, J. Cell Sci. 111 (1998) 373.
[43] R.I. Tuxworth, J.L. Cheetham, L.M. Machesky, G.B. Spiegelmann, G. Weeks, R.H. Insall, J. Cell Biol. 138 (1997) 605.
[44] H. Miike, S.C. Müller, B. Hess, Phys. Lett. A 141 (1989) 25.
[45] J.L. Podolski, T.L. Steck, J. Cell Biol. 265 (1990) 1312.
[46] K.M. Hedberg, T. Bengtsson, B. Safiejko-Mroczka, P.B.

Bell, M. Lindroth, Cell Motility Cytoskeleton 24 (1993) 139.
[47] S.-L. Li, Y. Miyata, I. Yahara, Y. Fujita-Yamaguchi, Exp. Cell Res. 205 (1993) 353.
[48] S. Yumura, Cell Struct. Func. 21 (1996a) 189.
[49] M. Westphal, A. Jungbluth, M. Heidecker et al., Curr. Biol. 7 (1997) 176.
[50] H. Aizawa, M. Sameshima, I. Yahara, Cell Struct. Func. 22 (1997b) 335.
[51] S. Yumura, Y. Fukui, J. Cell Sci. 111 (1998) 2097.
[52] M. Hellstén, U.P. Roos, Fung. Genet. Biol. 24 (1998) 123.
[53] M.H. Symons, T.J. Mitchison, J. Cell Biol. 114 (1991) 503.
[54] J.A. Theriot, T.J. Mitchison, Nature (London) 352 (1991) 126.
[55] J.A. Theriot, T.J. Mitchison, J. Cell Biol. 118 (1992) 367.
[56] C. Ballestrem, B. Wehrle-Haller, B.A. Imhof, J. Cell Sci. 111 (1998) 1649.
[57] M. Abercrombie, J.E. Heaysman, S.M. Pegrum, Exp. Cell Res. 60 (1970) 437.
[58] K. Gottmann, C.J. Weijer, J. Cell Biol. 102 (1986) 1623.
[59] S. Yumura, Protoplasma 192 (1996b) 217.
[60] P.A. Clow, J.G. McNally, Molec. Biol. Cell 16 (1999) 1309.
[61] A.J. Jesaitis, K.N. Klotz, Eur. J. Haematol. 51 (1993) 288.
[62] N. Barois, F. Forquet, J. Davoust, J. Cell Sci. 111 (1998) 1791.
[63] K.E. Parker, J. Physiol. (London) 510 (1998) 19.
[64] J.L.R. Freeman, E.M. Delacruz, T.D. Pollard, R.J. Lefkowitz, J.A. Pitcher, J. Biol. Chem. 273 (1998) 20653.
[65] P.A. Janmey, Physiol. Rev. 78 (1998) 763.
[66] A.L. Kindzelskii, M.M. Estes, R.F. Todd III, H.R. Petty, Biophys. J. 73 (1997) 777.
[67] A.L. Kindzelskii, M.-J. Zhou, R.P. Haugland, L.A. Boxer, H.R. Petty, Biophys. J. 74 (1998) 90.
[68] M.G. Vicker, W. Schill, K. Drescher, J. Cell Biol. 98 (1984) 2204.
[69] Y.-X. Li, A. Goldbeter, Biophys. J. 55 (1989) 125.
[70] C.A. Parent, P.N. Devreotes, Science 274 (1999) 765.
[71] M.G. Vicker, in: L. Rensing (Ed.), Oscillations Morphogenesis, Marcell Dekker, New York, 1993, p. 153.